Theoretical Study for Formation of Metal-oxo of First Transition Series with 14-TMC Ligand: Drives for "Oxo Wall"

Monika*[a], Manjeet Kumar[a], Somi[a], Arup Sarkar[b], Manoj Kumar Gupta[a] and Azaj Ansari*[a]

Email: monika.raoji@gmail.com and ajaz.alam2@gmail.com

[a]Department of Chemistry, Central University of Haryana, Mahendergarh, Haryana-123031, India.

[b]Department of Chemistry, The University of Chicago 5735 South Ellis Avenue, Chicago, IL 60637
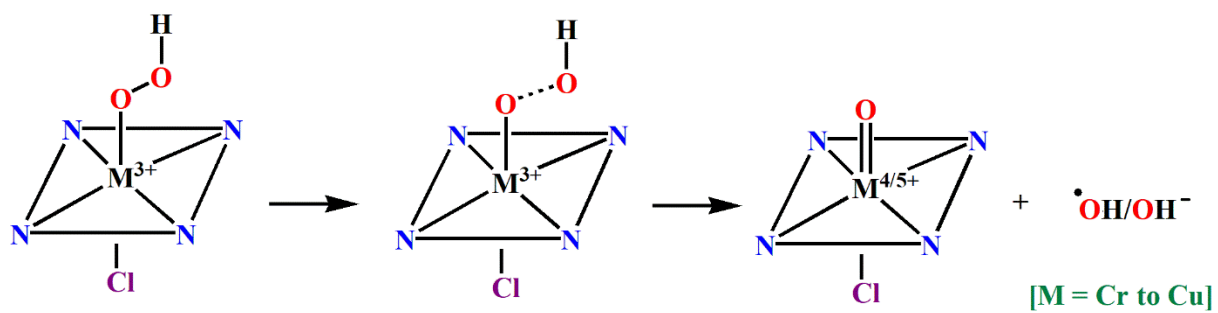
Scheme S1. Proposed mechanism for the formation of metal-oxo species.

Table S1. B3LYP-D2 computed relative energies in kJ/mol.

| Spin states	Energy (kJ/mol)	Spin states	Energy (kJ/mol)
$[(14\text{-TMC})(Cl)CrOOH]^+$		$[(14\text{-TMC})(Cl)MnOOH]^+$	
$^4Cr_{hs}$	0.0	$^5Mn_{hs}$	0.0
$^2Cr_{ls}$	157.0	$^3Mn_{is}$	46.8
		$^1Mn_{ls}$	144.8
$^4Cr_{hs}$-ts	74.8	$^5Mn_{hs}$-ts	66.3
$^2Cr_{ls}$-ts	150.5	$^3Mn_{is}$-ts	76.5
$^3Cr_{hs}$-Int	47.7	$^4Mn_{hs}$-Int	33.2
$^1Cr_{ls}$-Int	90.2	$^2Mn_{ls}$-Int	91.1
$[(14\text{-TMC})(Cl)FeOOH]^+$		$[(14\text{-TMC})(Cl)CoOOH]^+$	
$^6Fe_{hs}$	0.0	$^5Co_{hs}$	35.5
$^4Fe_{is}$	100.8	$^3Co_{is}$	25.8
$^2Fe_{ls}$	34.8	$^1Co_{ls}$	0.0
$^6Fe_{hs}$-ts	73.2	$^5Co_{hs}$-ts	99.8
$^4Fe_{is}$-ts	94.3		
$^2Fe_{ls}$-ts	83.8		
$^5Fe_{hs}$-Int	47.2	$^6Co_{hs}$-Int	142.7
$^3Fe_{is}$-Int	47.8	$^4Co_{is}$-Int	61.4
$^1Fe_{ls}$-Int	168.5	$^2Co_{ls}$-Int	71.5
$[(14\text{-TMC})(Cl)NiOOH]^+$		$[(14\text{-TMC})(Cl)CuOOH]^+$	
$^4Ni_{hs}$	-	$^3Cu_{hs}$	0.0
$^2Ni_{ls}$	0.0	$^1Cu_{ls}$	79.1
$^4Ni_{hs}$-ts	105.0	$^3Cu_{hs}$-ts	153.5
$^5Ni_{hs}$-Int	174.0	$^4Cu_{hs}$-Int	124.9
$^3Ni_{is}$-Int	246.6	$^2Cu_{ls}$-Int	155.5
$^1Ni_{ls}$-Int	-		
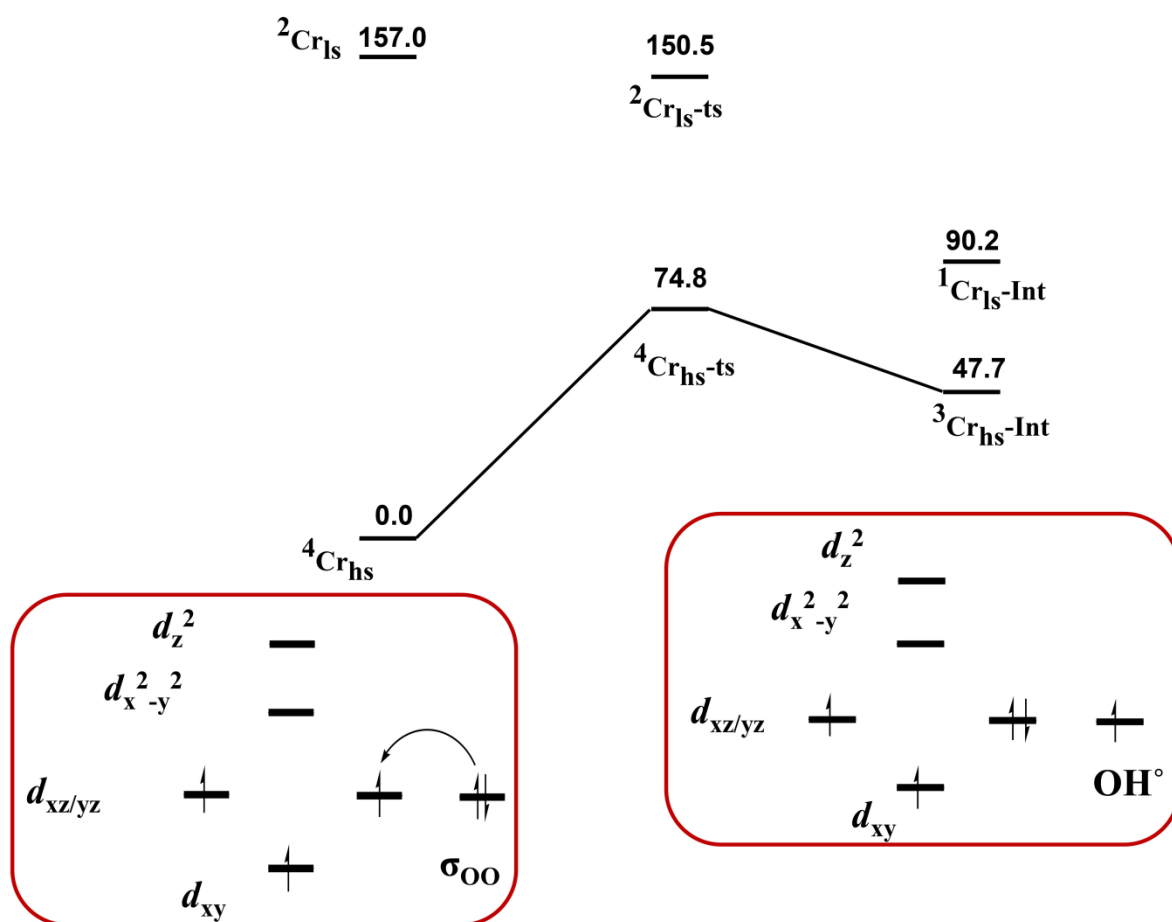
Figure S1. B3LYP-D2 computed energy surface (ΔG in kJ mol^{-1}) for the O---O bond cleavage of chromium(III) hydroperoxo species.

(a)

O2

1.515

N4   O1   N3

1.943

Cr

N1   N2

2.398

Cl

Cr-N$_{avg}$ = 2.173 Å
∠ Cl-Cr-O1 = 172.0°
∠ Cr-O1-O2 = 127.5°

(b)

O2

2.368

N4   O1   N3

1.725

Cr

N1   N2

2.409

Cl

Cr-N$_{avg}$ = 2.172 Å
∠ Cl-Cr-O1 = 175.6°
∠ Cr-O1-O2 = 142.5°
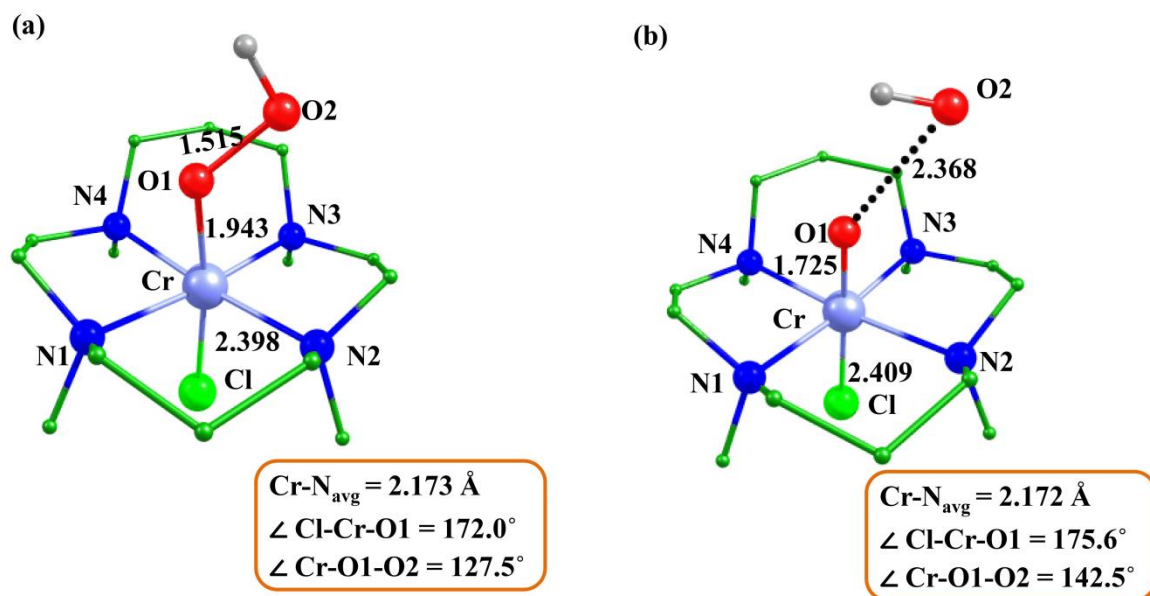
Figure S2. B3LYP-D2 a) optimized structure of the ground state of chromium hydroperoxo (^{4}Cr$_{hs}$); (b) optimized structure of the ground state of transition state ^{4}Cr$_{hs}$-ts (bond lengths are in Å).

Table S2. B3LYP-D2 computed selected structural parameters of the 14-TMC metal hydroperoxo species, transition states (O---O) and metal-oxo.

Spin State	Bond length (Å)								Bond Angle (°)				
	M-O	M-N$_1$	M-N$_2$	M-N$_3$	M-N$_4$	M-N avg	M-Cl	O-O	Cl-M-O	M-O-O	O-O-H	N$_1$-M-N$_3$	N$_2$-M-N$_4$
[(14-TMC)(Cl)CrOOH]$^+$													
^{4}Cr$_{hs}$	1.943	2.147	2.183	2.196	2.161	2.173	2.398	1.515	172.0	127.5	99.7	175.0	174.6
^{2}Cr$_{ls}$	1.894	2.161	2.146	2.185	2.197	2.171	2.386	1.518	171.9	129.2	99.6	175.3	174.9
^{4}Cr$_{hs}$-ts	1.725	2.189	2.159	2.164	2.175	2.172	2.409	2.368	175.6	142.5	68.9	174.8	174.8
^{2}Cr$_{ls}$-ts	1.686	2.205	2.163	2.138	2.188	2.173	2.389	1.878	172.8	137.0	89.9	176.6	175.8
^{3}Cr$_{hs}$-Int	1.715	2.167	2.167	2.176	2.176	2.171	2.419	-	176.8	-	-	174.5	174.5
^{1}Cr$_{ls}$-Int	1.580	2.182	2.181	2.175	2.175	2.178	2.387		176.9	-	-	176.6	176.6
Exp.^{1}	1.618												
[(14-TMC)(Cl)MnOOH]$^+$													
^{5}Mn$_{hs}$	1.916	2.132	2.318	2.179	2.313	2.236	2.344	1.511	169.9	127.8	99.6	173.7	173.7
^{3}Mn$_{is}$	1.885	2.117	2.162	2.175	2.130	2.146	2.351	1.519	171.2	127.1	99.3	175.8	175.3
^{1}Mn$_{ls}$	1.767	2.127	2.173	2.184	2.135	2.155	2.343	1.537	170.8	130.1	99.1	176.7	176.3
^{5}Mn$_{hs}$-ts	1.748	2.171	2.153	2.140	2.158	2.156	2.433	1.854	176.8	156.5	92.6	174.0	174.2
^{3}Mn$_{is}$-ts	1.723	2.106	2.160	2.179	2.122	2.142	2.393	1.852	171.6	130.7	89.2	176.6	175.8
^{4}Mn$_{hs}$-Int	1.680	2.134	2.157	2.134	2.157	2.145	2.417	-	177.7	-	-	175.1	175.1
^{2}Mn$_{ls}$-Int	1.637	2.143	2.154	2.143	2.153	2.148	2.370	-	177.1	-	-	175.6	175.5
[(14-TMC)(Cl)FeOOH]$^+$													
^{6}Fe$_{hs}$	1.953	2.209	2.229	2.247	2.231	2.249	2.378	1.495	173.5	134.8	101.1	173.0	172.4
^{4}Fe$_{is}$	2.021	2.124	2.166	2.151	2.156	2.154	2.457	1.514	130.6	130.6	100.8	174.6	174.3
^{2}Fe$_{ls}$	1.858	2.137	2.157	2.107	2.109	2.127	2.344	1.522	171.4	126.5	99.3	176.5	175.9
^{6}Fe$_{hs}$-ts	1.677	2.242	2.235	2.209	2.197	2.221	2.322	2.052	177.1	157.7	88.2	172.8	172.5
^{4}Fe$_{is}$-ts	1.718	2.137	2.150	2.140	2.124	2.139	2.385	1.822	177.1	159.3	93.9	174.9	174.7
^{2}Fe$_{ls}$-ts	1.675	2.098	2.138	2.157	2.111	2.126	2.351	2.019	173.8	136.5	83.7	176.7	176.1
^{5}Fe$_{hs}$-Int	1.659	2.202	2.202	2.238	2.237	2.219	2.327	-	177.5	-	-	173.4	173.4
^{3}Fe$_{is}$-Int	1.657	2.195	2.235	2.207	2.242	2.219	2.362	-	178.1	-	-	175.4	175.4
^{1}Fe$_{ls}$-Int	1.669	2.119	2.119	2.128	2.128	2.123	2.346	-	176.9	-	-	175.3	175.3

Exp.[2]	1.646	-	-	2.067	2.069	2.109	2.117	-	-	-	-	-	-
[(14-TMC)(Cl)CoOOH]+													
$^5Co_{hs}$	1.984	2.180	2.221	2.216	2.209	2.206	2.415	1.472	171.4	132.1	102.3	174.0	173.3
$^3Co_{is}$	1.917	2.063	2.243	2.117	2.235	2.164	2.384	1.511	172.0	128.6	100.1	175.6	175.2
$^1Co_{ls}$	1.934	2.073	2.114	2.133	2.080	2.100	2.342	1.525	171.2	123.8	99.3	176.2	175.7
$^5Co_{hs}$-ts	1.674	2.226	2.226	2.212	2.212	2.219	2.286	1.921	176.2	162.5	92.3	173.1	173.1
$^6Co_{hs}$-Int	1.872	2.221	2.225	2.221	2.226	2.223	2.374	-	174.4	-	-	170.9	170.9
$^4Co_{is}$-Int	1.647	2.199	2.221	2.199	2.221	2.210	2.284	-	177.5	-	-	173.9	173.8
$^2Co_{ls}$-Int	1.835	2.090	2.098	2.090	2.099	2.094	2.353	-	177.4	-	-	173.7	173.7
Exp.[3-4]	1.72												
[(14-TMC)(Cl)NiOOH]+													
$^2Ni_{ls}$	2.013	2.148	2.211	2.198	2.196	2.189	2.341	1.459	171.1	128.2	103.2	173.8	173.7
$^4Ni_{hs}$-ts	1.836	2.208	2.162	2.192	2.172	2.183	2.284	2.072	176.2	154.1	96.0	171.7	171.8
$^5Ni_{hs}$-Int	1.838	2.218	2.196	2.197	2.218	2.207	2.376	-	174.8	-	-	172.2	172.2
$^1Ni_{ls}$-Int	1.853	2.174	2.173	2.184	2.184	2.179	2.289	-	177.1	-	-	171.5	171.5
[(14-TMC)(Cl)CuOOH]+													
$^3Cu_{hs}$	2.291	2.150	2.181	2.177	2.183	2.173	2.501	1.455	171.9	130.8	104.7	171.1	171.5
$^1Cu_{hs}$	1.919	2.207	2.328	2.254	2.326	2.279	2.262	1.475	168.1	125.5	102.8	174.0	174.4
$^3Cu_{hs}$-ts	2.004	2.242	2.190	2.228	2.218	2.219	2.358	2.036	175.4	135.5	85.4	171.4	171.4
$^4Cu_{hs}$-Int	2.031	2.189	2.190	2.188	2.188	2.189	2.420	-	176.3	-	-	170.5	170.5
$^2Cu_{ls}$-Int	2.083	2.183	2.184	2.177	2.178	2.180	2.448	-	176.4	-	-	170.3	170.3

Table S3. B3LYP-D2 computed selected spin density values of the 14-TMC species, transition states, and metal-oxo.

Spin state	Metal	O1	O2
$[(14\text{-}TMC)(Cl)CrOOH]^+$			
$^4Cr_{hs}$	3.179	-0.001	0.040
$^2Cr_{ls}$	1.126	-0.045	0.007
$^4Cr_{hs}$-ts	2.812	-0.513	0.961
$^2Cr_{ls}$-ts	0.697	-0.281	0.663
$^3Cr_{hs}$-Int	2.784	-0.569	-
$^1Cr_{ls}$-Int	0	0	-
$[(14\text{-}TMC)(Cl)MnOOH]^+$			
$^5Mn_{hs}$	3.987	-0.010	0.042
$^3Mn_{is}$	2.098	0.042	0.023
$^1Mn_{ls}$	0.000	0.000	0.000
$^5Mn_{hs}$-ts	3.341	0.269	0.668
$^3Mn_{is}$-ts	2.493	0.272	-0.549
$^4Mn_{hs}$-Int	2.677	0.545	-
$^2Mn_{ls}$-Int	1.165	-0.061	-
$[(14\text{-}TMC)(Cl)FeOOH]^+$			
$^6Fe_{hs}$	3.980	0.277	0.051
$^4Fe_{is}$	2.896	0.194	0.030
$^2Fe_{ls}$	1.039	0.089	-0.000
$^6Fe_{hs}$-ts	3.275	0.528	0.869
$^4Fe_{is}$-ts	2.352	-0.151	0.0058
$^2Fe_{ls}$-ts	1.309	0.575	-0.775
$^5Fe_{hs}$-Int	3.081	0.632	-
$^3Fe_{is}$-Int	1.313	0.793	-
$^1Fe_{ls}$-Int	0	0	-
$[(14\text{-}TMC)(Cl)CoOOH]^+$			
$^5Co_{hs}$	2.776	0.437	0.083
$^3Co_{is}$	1.829	0.173	0.013
$^1Co_{ls}$	0.000	0.000	0.000
$^5Co_{hs}$-ts	2.164	0.673	0.798
$^6Co_{hs}$-Int	2.750	1.400	-
$^4Co_{is}$-Int	1.855	0.884	-
$^2Co_{ls}$-Int	-0.026	0.974	-
$[(14\text{-}TMC)(Cl)NiOOH]^+$			
$^2Ni_{ls}$	1.277	-0.099	-0.344
$^4Ni_{hs}$-ts	0.936	0.928	0.853

|			
$^5Ni_{hs}$-Int	1.545	1.571	-
$^3Ni_{is}$-Int	0.957	-1.156	-
	$[(14\text{-}TMC)(Cl)CuOOH]^+$		
$^3Cu_{hs}$	0.519	0.474	0.123
$^1Cu_{ls}$	0.000	0.000	0.000
$^3Cu_{hs}$-ts	0.030	1.231	0.796
$^4Cu_{hs}$-Int	0.534	1.362	-
$^2Cu_{ls}$-Int	-0.165	1.425	-
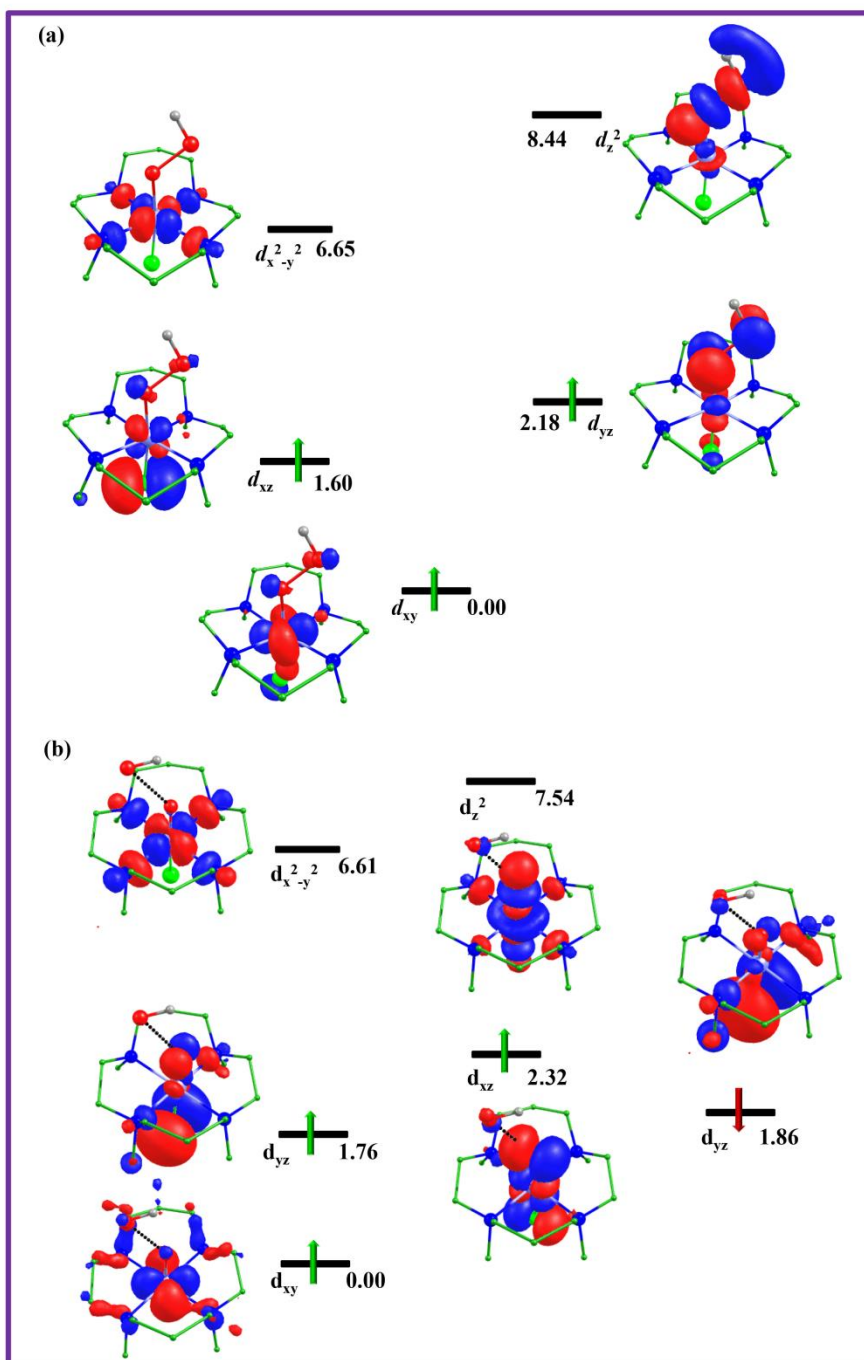
Figure S3. Computed eigenvalue plot incorporating energies computed for d-based orbitals for alpha corresponding to the ground state a) ^{4}Cr$_{hs}$; b) ^{4}Cr$_{hs}$-ts of the chromium(III) hydroperoxo species (energies are given in eV).

(^{4}Cr$_{hs}$)

$d_{xy}(1.00e^-)$ $d_{xz}(1.00e^-)$ $d_{yz}(1.00e^-)$ $d_{x^2-y^2}(0.14e^-)$ $d_{z^2}(0.14e^-)$

(^{4}Cr$_{hs}$-ts)

$d_{xy}(1.00e^-)$ $d_{xz}(1.00e^-)$ $d_{yz}(1.00e^-)$ $d_{x^2-y^2}(0.14e^-)$ $d_{z^2}(0.00e^-)$ $d_{yz}(-0.64e^-)$
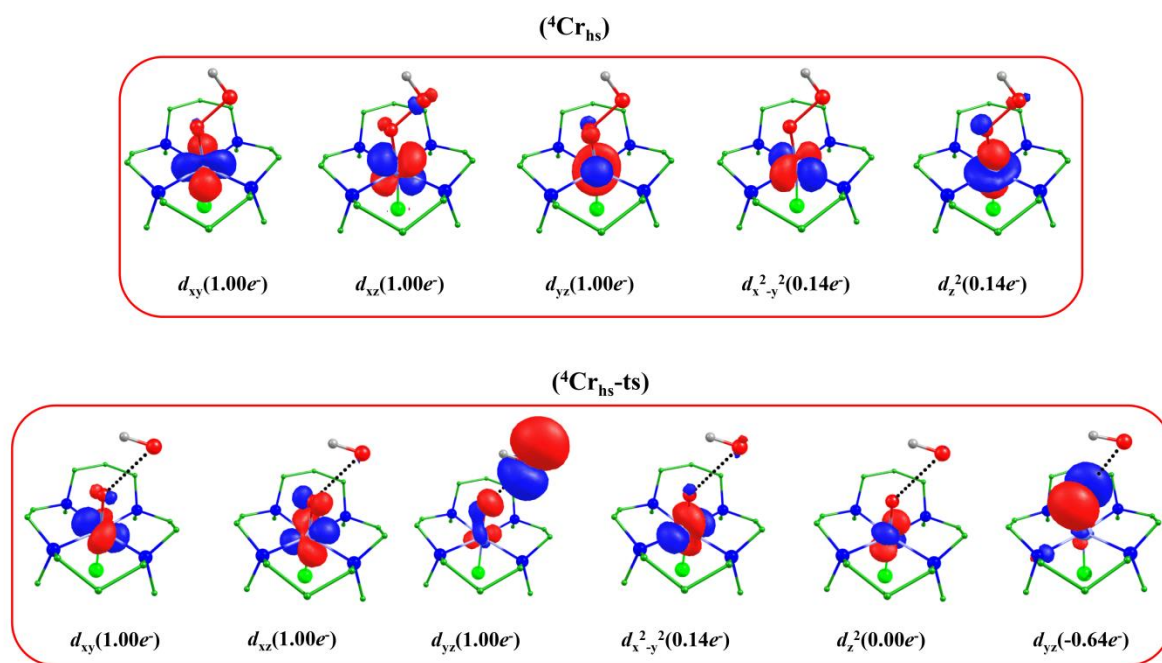
Figure S4. Spin natural orbitals and their occupations (noted in parenthesis) of ^{4}Cr$_{hs}$, and ^{4}Cr$_{hs}$-ts.

Table S4. Computed Wiberg bond indices of chromium-copper species.

Spin State	M-O	O1-O2
$[(14\text{-TMC})(\text{Cl})\text{CrOOH}]^+$		
$^4\text{Cr}_{hs}$	0.218	0.246
$^4\text{Cr}_{hs}\text{-ts}$	0.374	0.054
$^3\text{Cr}_{hs}\text{-Int}$	0.403	-
$[(14\text{-TMC})(\text{Cl})\text{MnOOH}]^+$; II Species		
$^5\text{Mn}_{hs}$	0.198	0.245
$^5\text{Mn}_{hs}\text{-ts}$	0.443	0.180
$^4\text{Mn}_{hs}\text{-Int}$	0.624	-
$[(14\text{-TMC})(\text{Cl})\text{FeOOH}]^+$; III Species		
$^6\text{Fe}_{hs}$	0.260	0.249
$^4\text{Fe}_{is}\text{-ts}$	0.556	0.107
$^5\text{Fe}_{hs}\text{-Int}$	0.631	-
$[(14\text{-TMC})(\text{Cl})\text{CoOOH}]^+$; IV Species		
$^1\text{Co}_{ls}$	0.152	0.244
$^5\text{Co}_{hs}$	0.539	0.147
$^4\text{Co}_{is}\text{-Int}$	0.640	-
$[(14\text{-TMC})(\text{Cl})\text{NiOOH}]^+$; V Species		
$^2\text{Ni}_{ls}$	0.101	0.246
$^4\text{Ni}_{hs}\text{-ts}$	0.202	0.143
$^2\text{Ni}_{ls}$	0.423	-
$[(14\text{-TMC})(\text{Cl})\text{CuOOH}]^+$; VI Species		
$^3\text{Cu}_{hs}$	0.106	0.306
$^3\text{Cu}_{hs}\text{-ts}$	0.158	0.088
$^4\text{Cu}_{hs}\text{-Int}$	0.177	-

144.8

^{1}Mn$_{ls}$

^{3}Mn$_{is}$-ts

76.5

91.1

^{2}Mn$_{ls}$-Int

46.8

^{3}Mn$_{is}$

66.3

^{5}Mn$_{hs}$-ts

33.2

^{4}II$_{hs}$-Int

0.0

^{5}Mn$_{hs}$

d_z^2

$d_{x^2-y^2}$

$d_{xz/yz}$

OH°

d_{xy}

d_z^2

$d_{x^2-y^2}$

$d_{xz/yz}$

d_{xy}

σ_{OO}
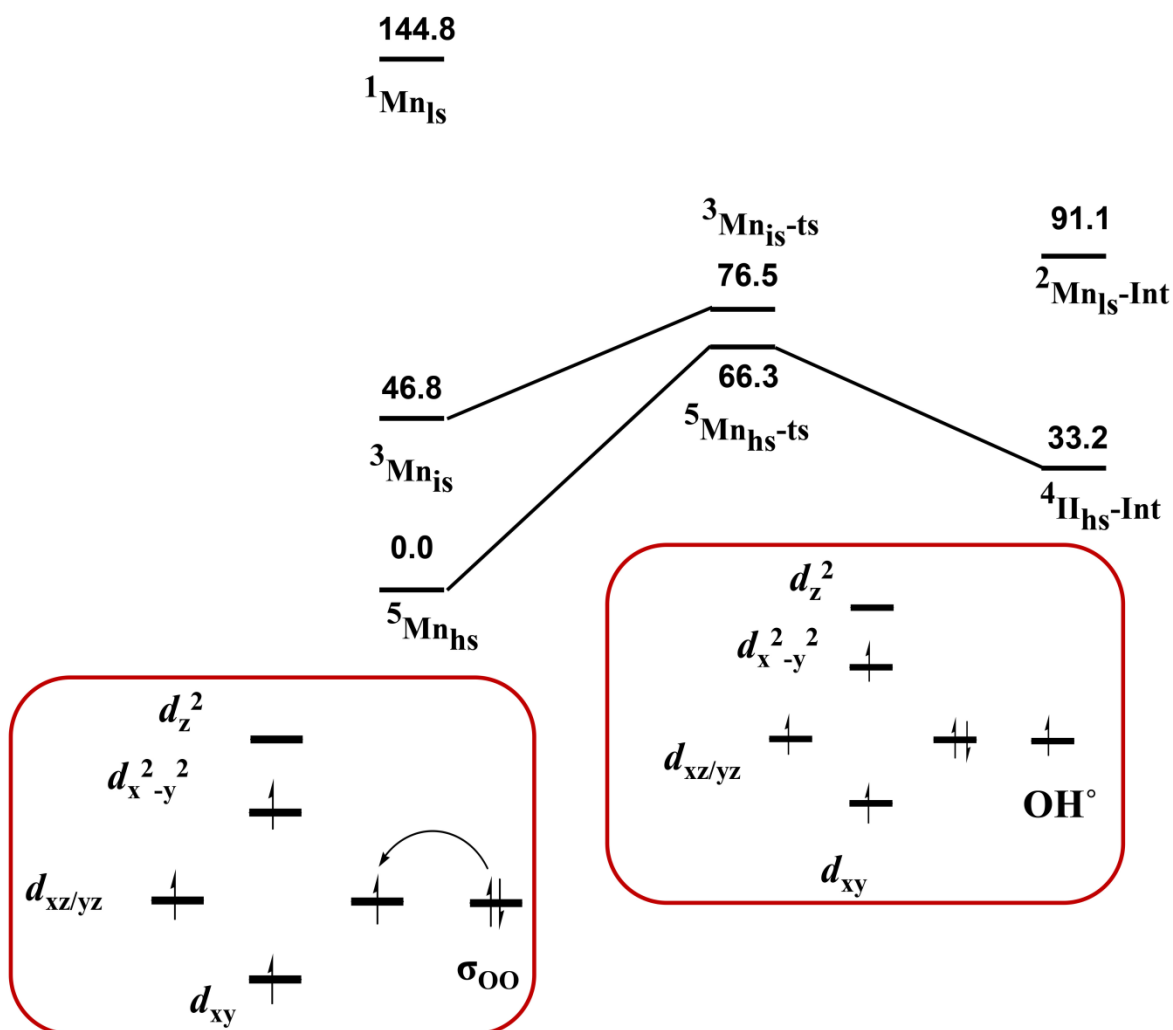
Figure S5. B3LYP-D2 computed energy surface (ΔG in kJ mol^{-1}) for the O---O bond cleavage of manganese hydroperoxo species.
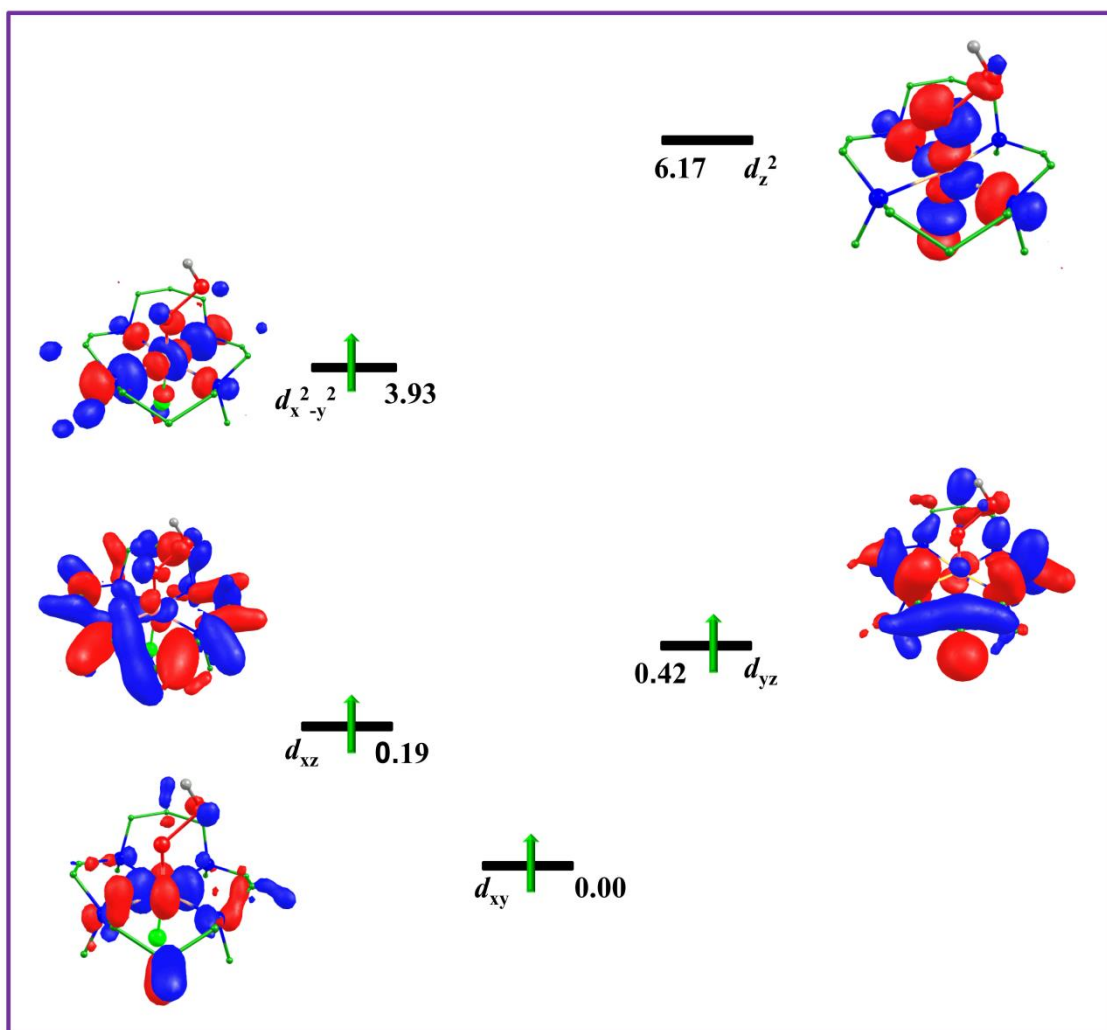
Figure S6. Computed eigenvalue plot incorporating energies computed for d-based orbitals for alpha spin corresponding to the ground state $^5Mn_{hs}$ of the manganese hydroperoxo species (energies are given in eV).

$^5Mn_{hs}$

$d_{xy}(1.00e^-)$ $d_{xz}(1.00e^-)$ $d_{yz}(1.00e^-)$ $d_{x^2-y^2}(1.00e^-)$ $d_{z^2}(0.30e^-)$

$^5Mn_{hs}$-ts

$d_{xy}(1.00e^-)$ $d_{xz}(1.00e^-)$ $d_{yz}(1.00e^-)$ $d_{x^2-y^2}(0.27e^-)$ $d_{z^2}(1.00e^-)$ $d_{xz}(-0.26e^-)$
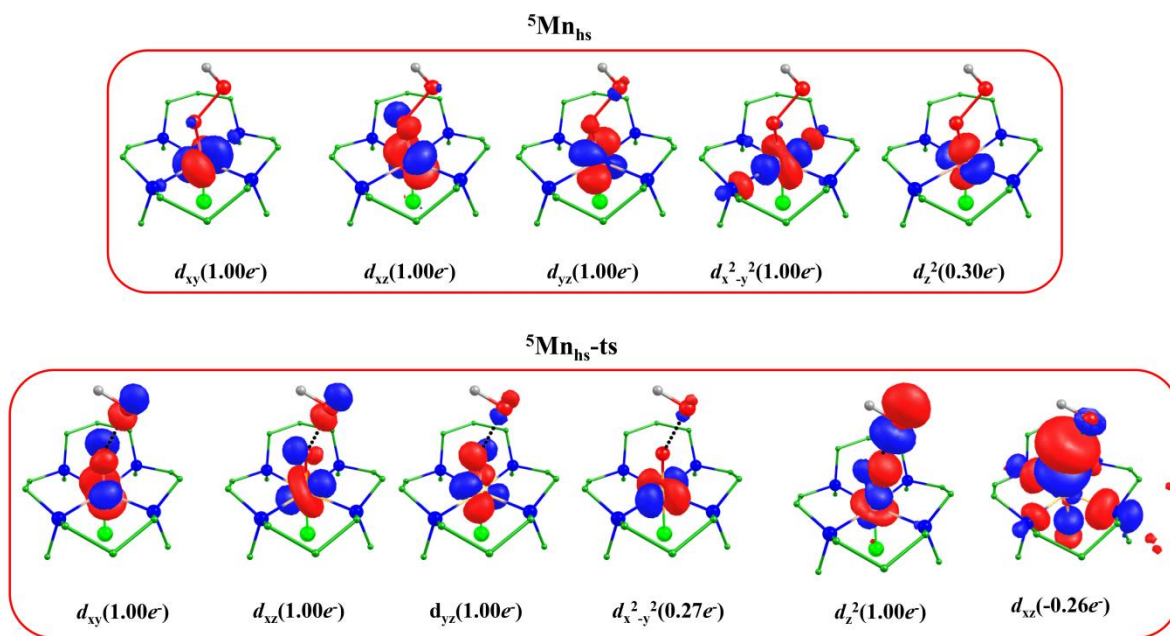
Figure S7. Spin natural orbitals and their occupations (noted in parenthesis) of $^5Mn_{hs}$, and $^5Mn_{hs}$-ts.
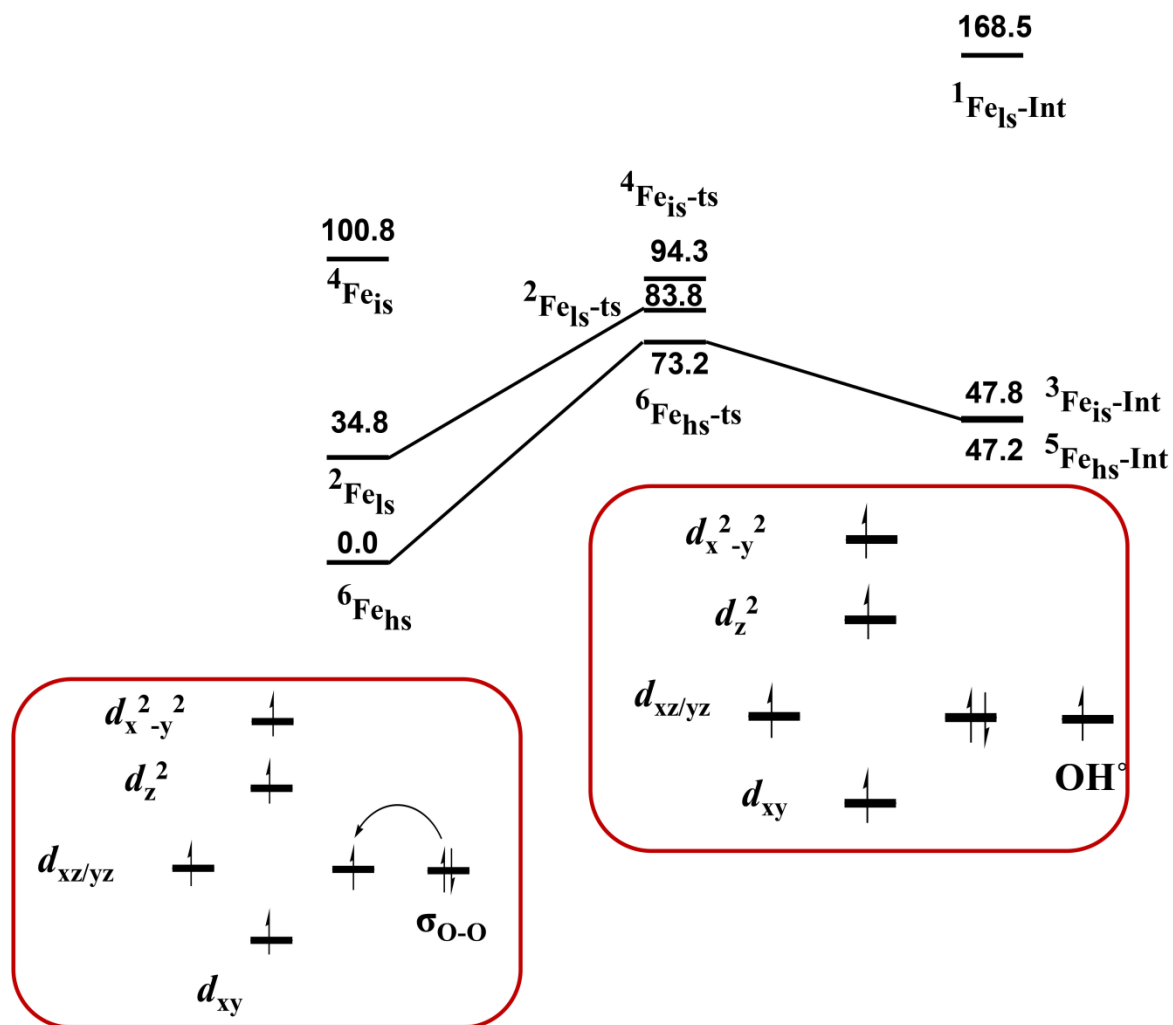
Figure S8. B3LYP-D2 computed energy surface (ΔG in kJ mol^{-1}) for the O---O bond cleavage of iron(III) hydroperoxo species.

(a)

(b)

1.495

O2

O1   1.953

N4   N3

Fe

N1   N2

2.378

Cl

Fe-N$_{avg}$ = 2.249 Å
∠ Cl-Fe-O1 = 173.5°
∠ Fe-O1-O2 = 134.8°

2.052

O2

O1   1.677

N4   N3

Fe

N1   N2

2.322

Cl

Fe-N$_{avg}$ = 2.221 Å
∠ Cl-Fe-O1 = 177.1°
∠ Fe-O1-O2 = 157.7°

(c)

0.277

3.980

(^{6}Fe$_{hs}$)

0.869

0.528

3.275
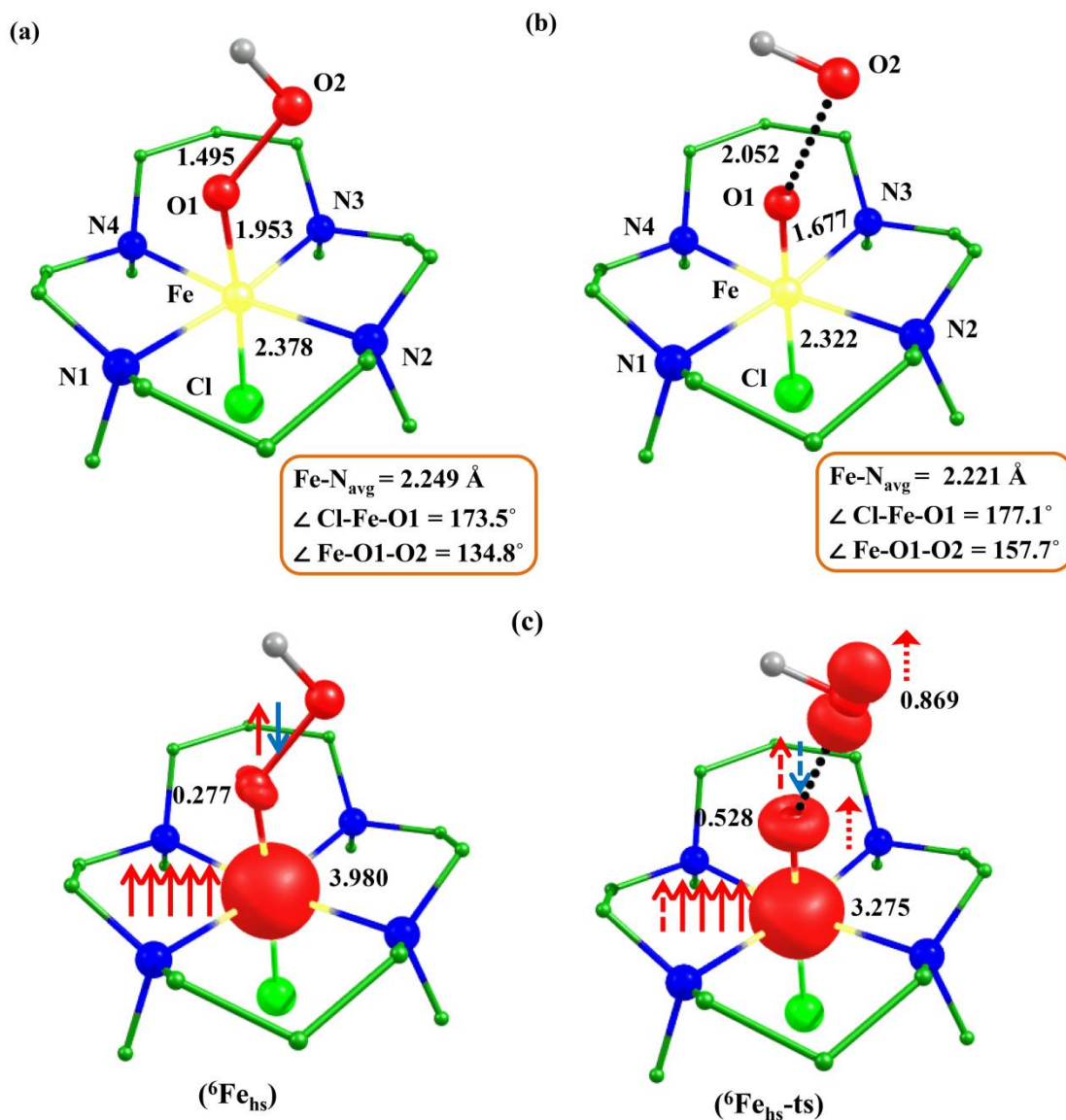
(^{6}Fe$_{hs}$-ts)

Figure S9. B3LYP-D2 (a) optimized structure of the ground state of iron(III) hydroperoxo (^{6}Fe$_{hs}$); (b) optimized structure of the ground state of the transition state of iron(III) hydroperoxo (^{6}Fe$_{hs}$-ts); (c) scheme for the formation of π bond between iron and oxygen center by the involvement of O-O bond electrons and iron center.
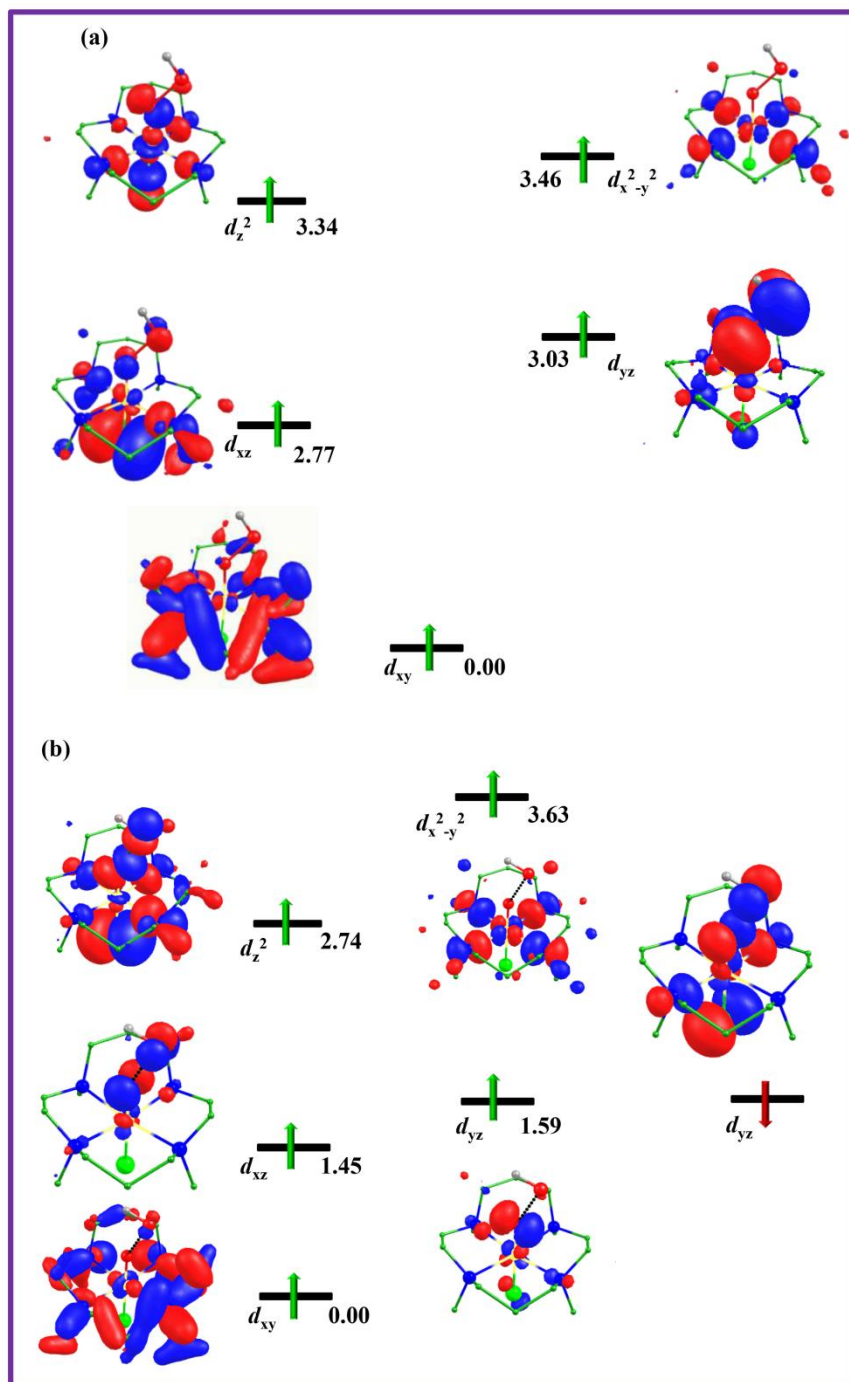
Figure S10. Computed eigenvalue plot incorporating energies computed for d-based orbitals for alpha spin corresponding to the ground state of the iron(III) hydroperoxo a) $^6Fe_{hs}$; b) $^6Fe_{hs}$-ts (energies are given in eV).
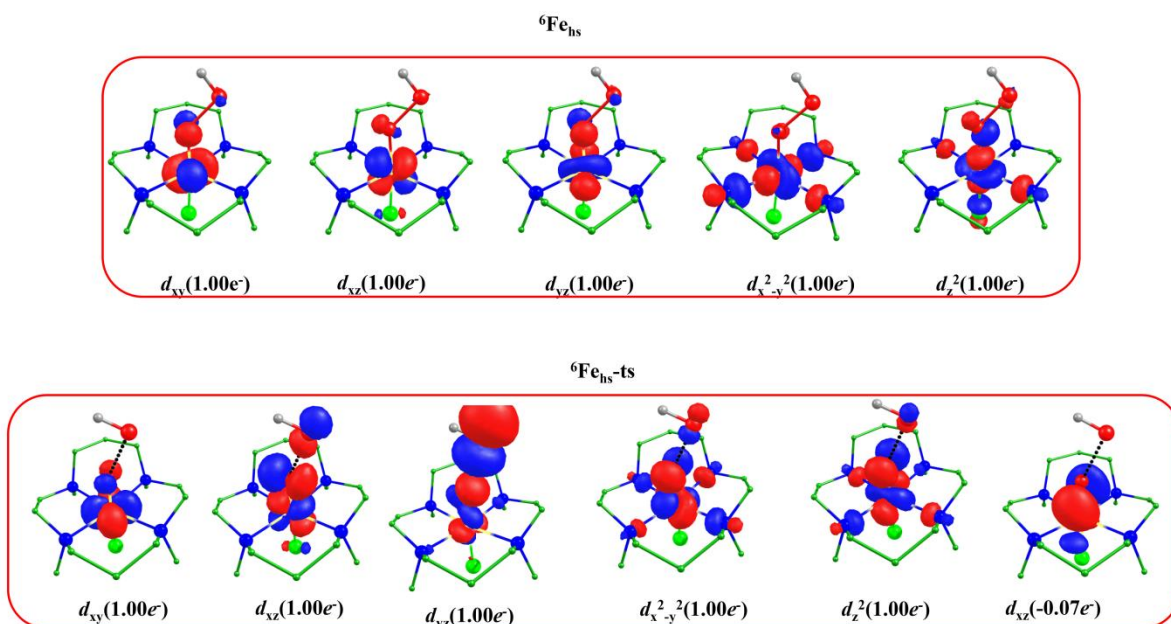
Figure S11. Spin natural orbitals and their occupations (noted in parenthesis) of $^6\text{Fe}_{hs}$, and $^6\text{Fe}_{hs}$-ts.
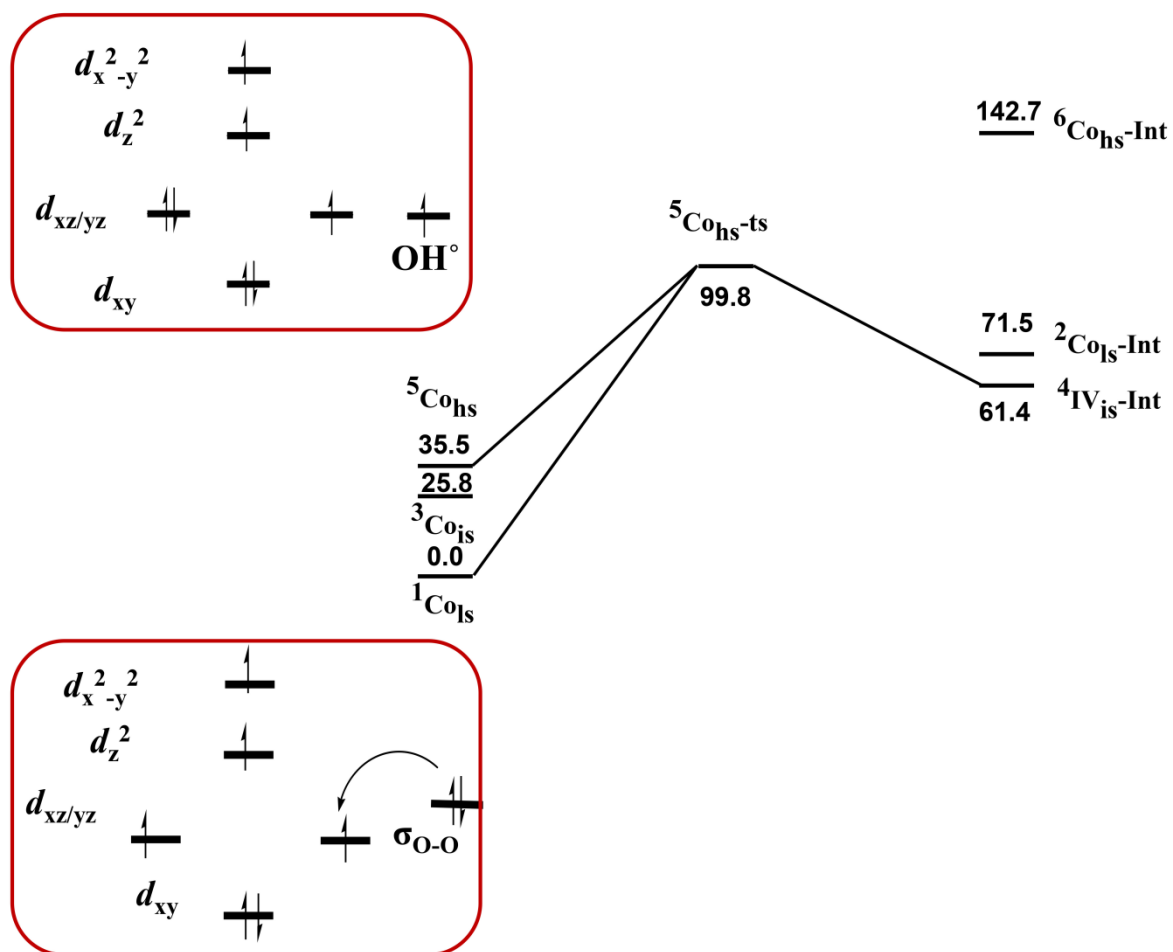
Figure S12. B3LYP-D2 computed energy surface (ΔG in kJ mol^{-1}) for the O---O bond cleavage of cobalt(III) hydroperoxo species.
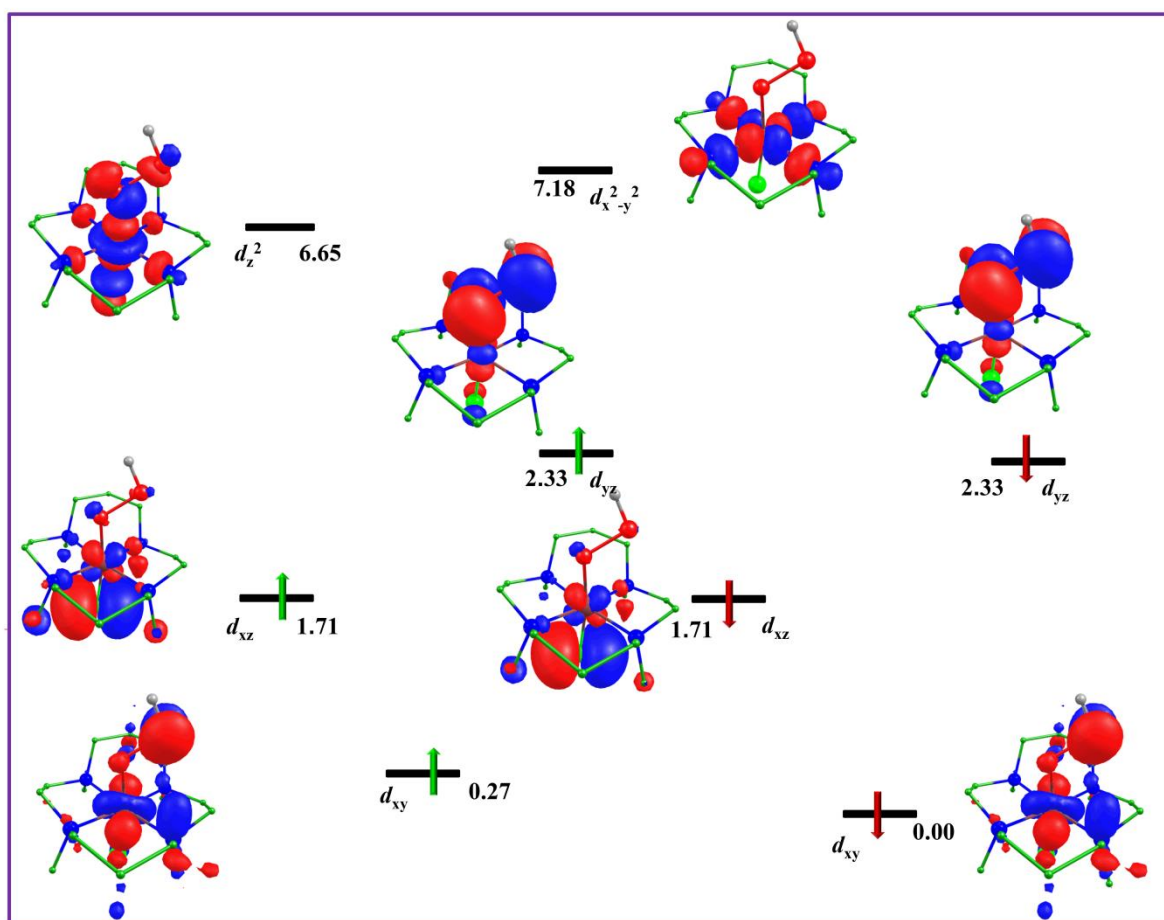
Figure S13. Computed eigenvalue plot incorporating energies computed for d-based orbitals for alpha and beta spin corresponding to the ground state $^1Co_{ls}$ of the cobalt(III) hydroperoxo species (energies are given in eV).
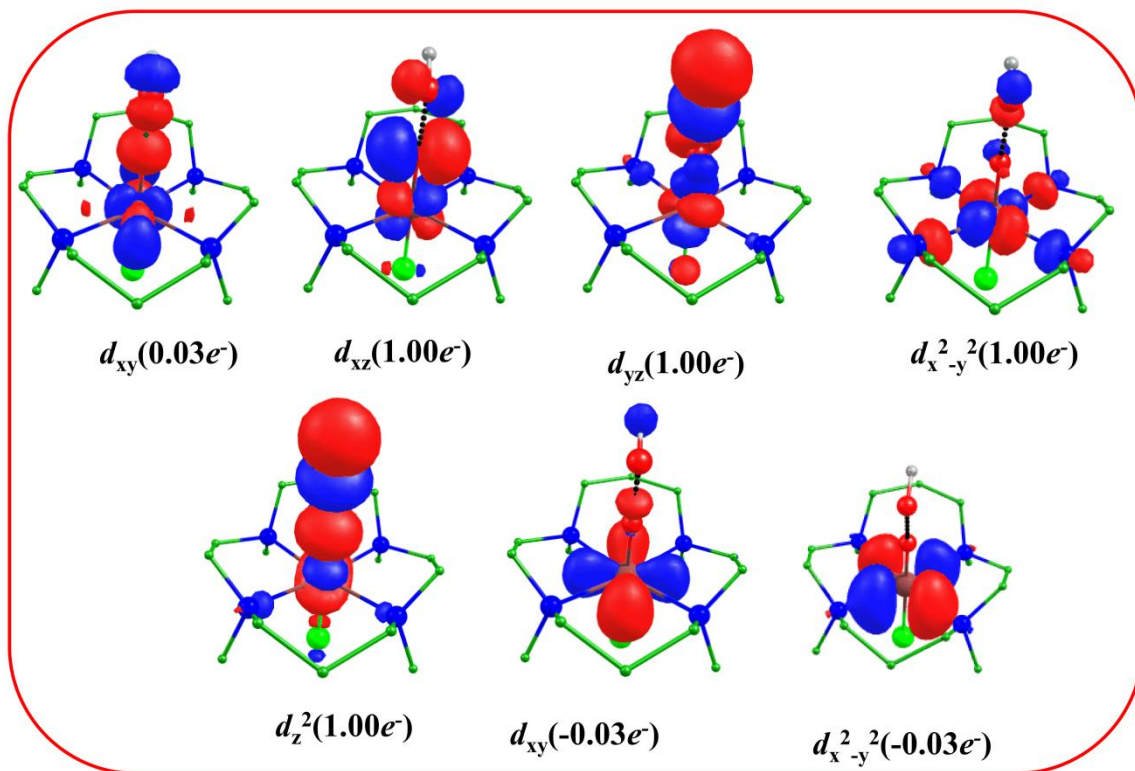
Figure S14. Spin natural orbitals and their occupations (noted in parenthesis) of $^5Co_{hs}$-ts.
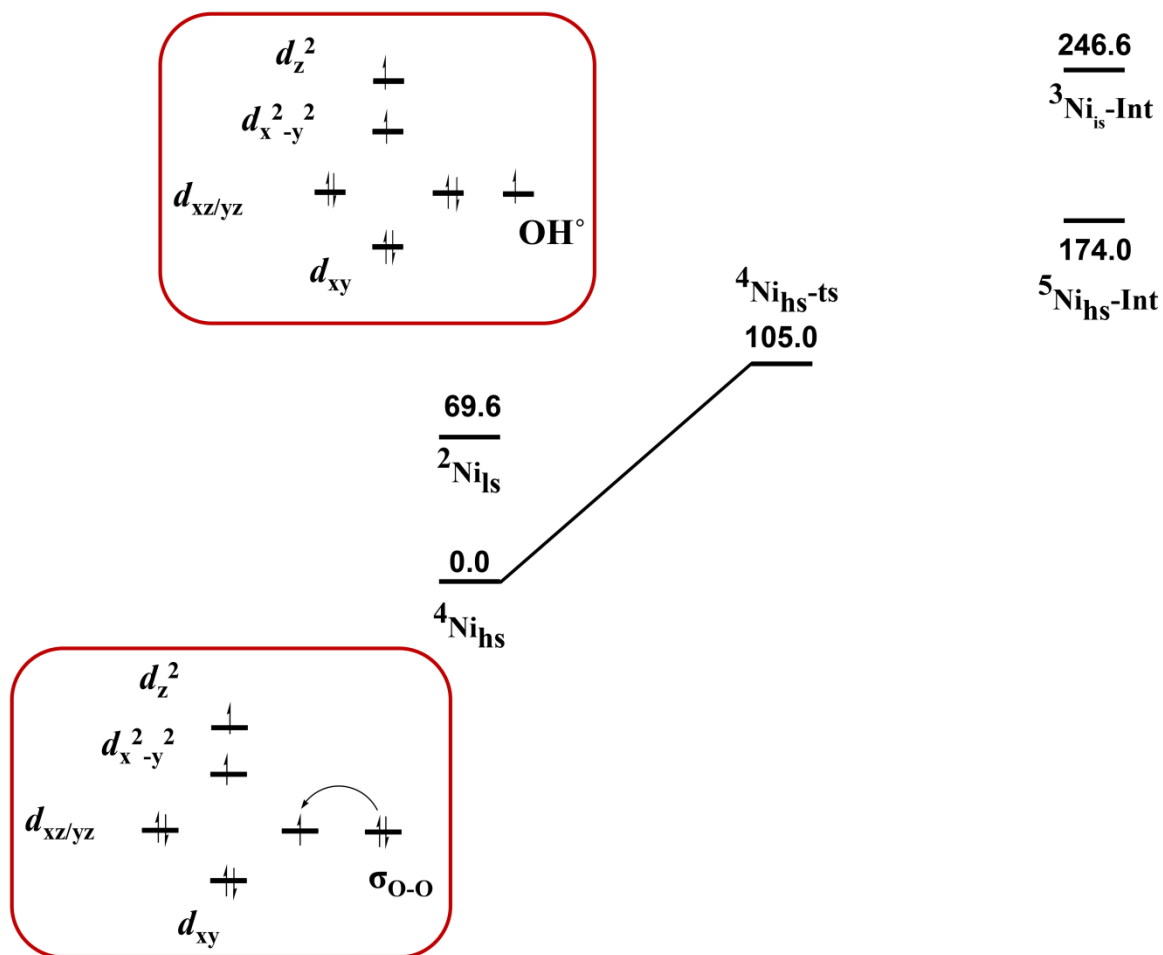
Figure S15. B3LYP-D2 computed energy surface (ΔG in kJ mol^{-1}) for the O---O bond cleavage of nickel(III) hydroperoxo.
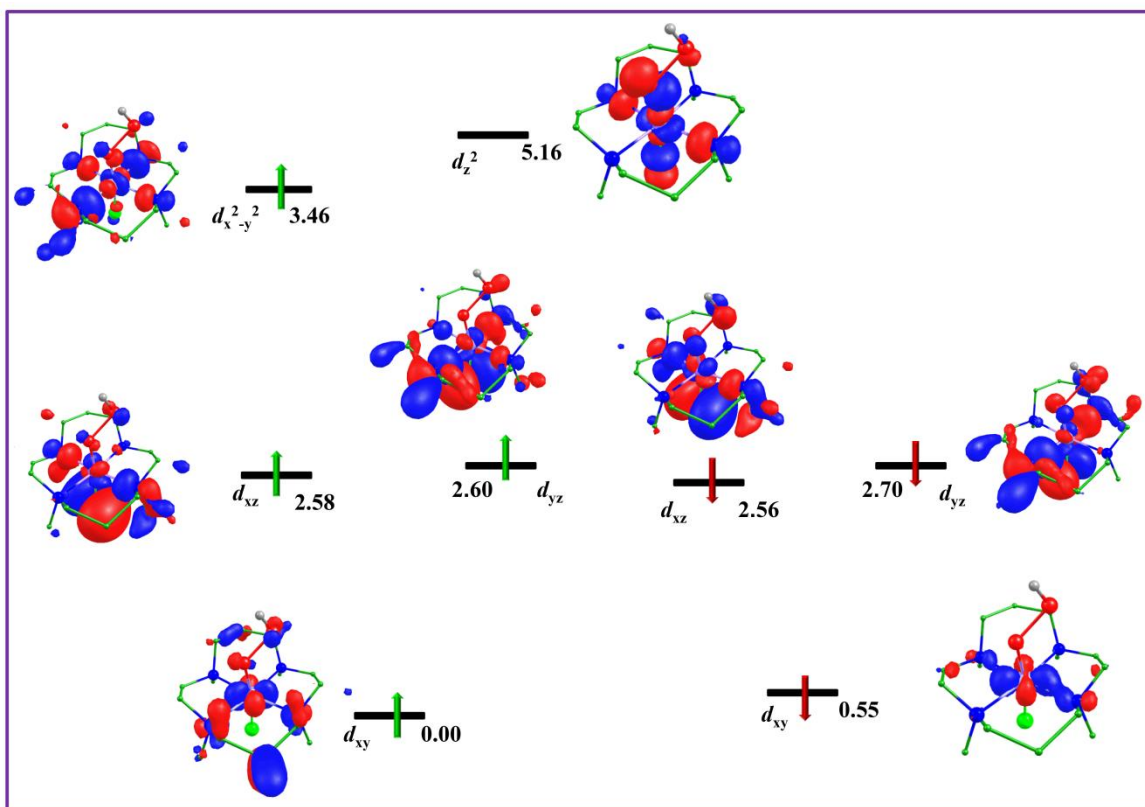
Figure S16. Computed eigenvalue plot incorporating energies computed for *d*-based orbitals for alpha and beta spin corresponding to the ground state $^2Ni_{ls}$ of the species V(energies are given in eV).
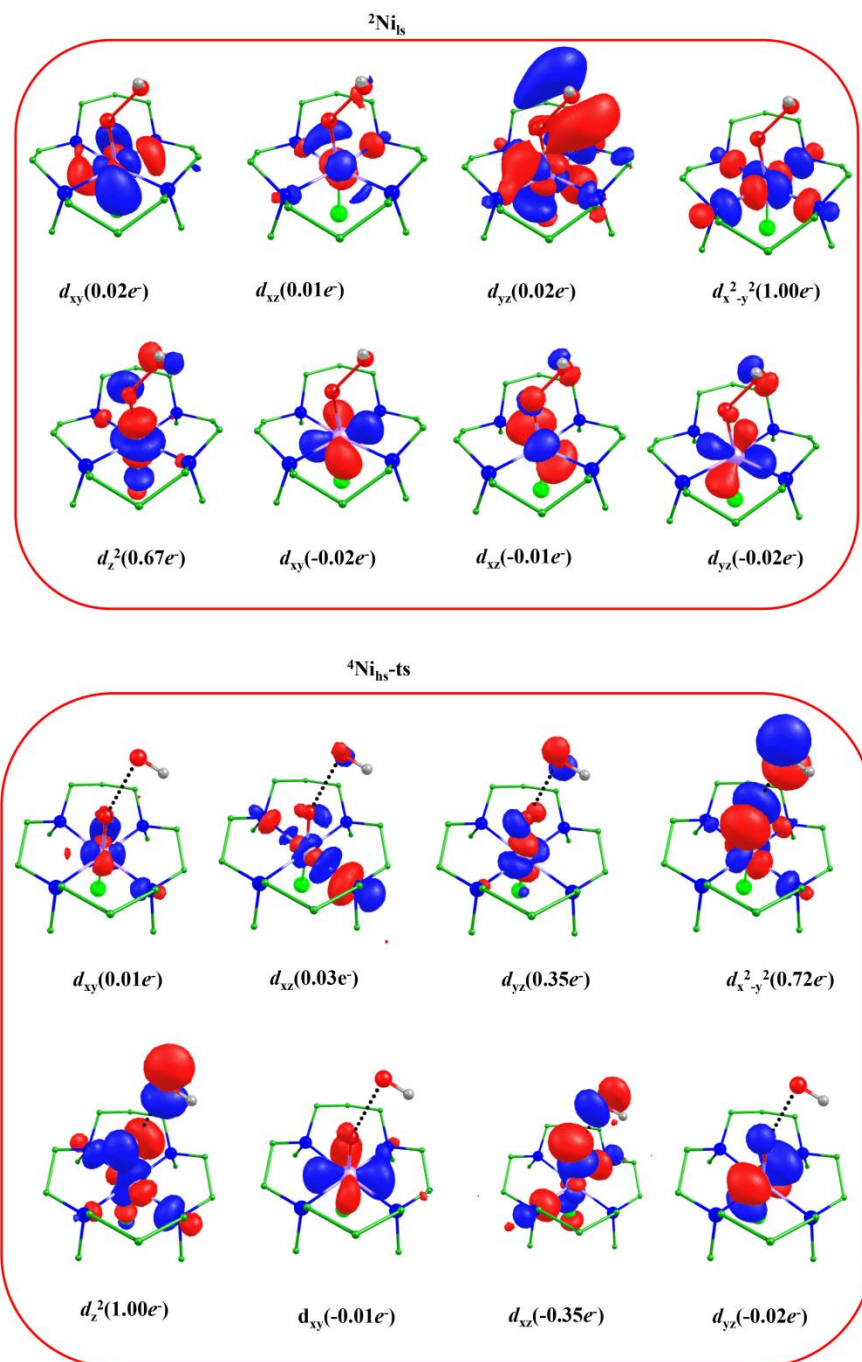
Figure S17. Spin natural orbitals and their occupations (noted in parenthesis) of $^2Ni_{ls}$ and $^4Ni_{hs}$-ts of species V.
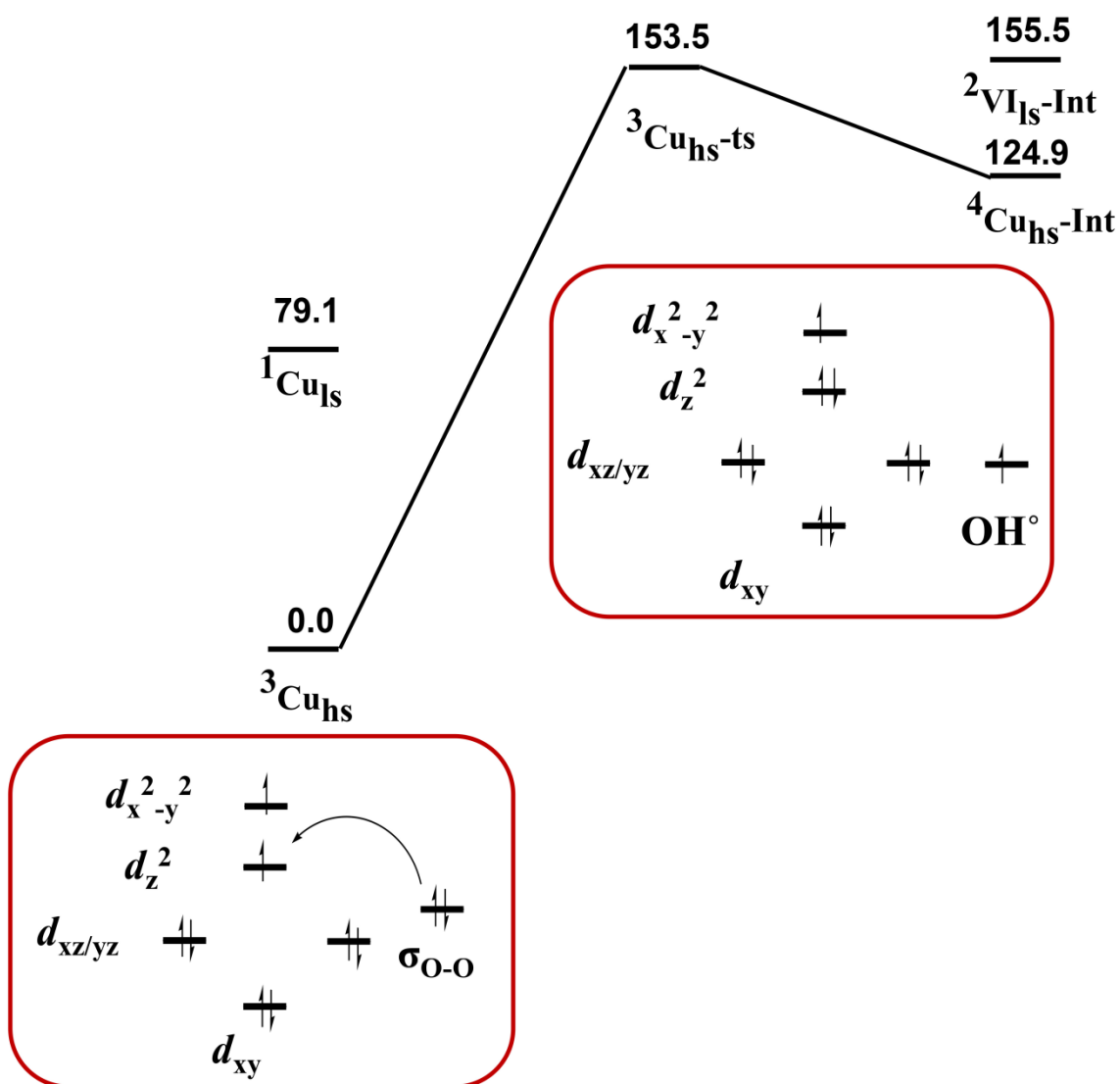
Figure S18. B3LYP-D2 computed energy surface (ΔG in kJ mol^{-1}) for the O---O bond cleavage of copper(III) hydroperoxo species.
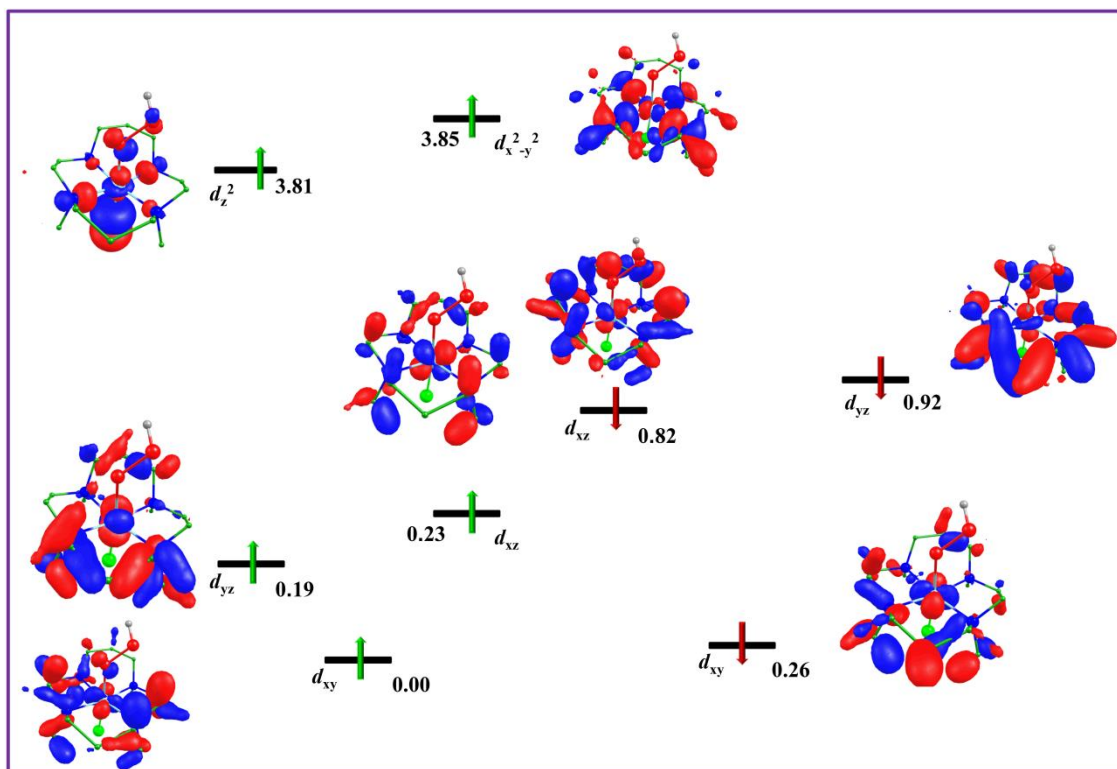
Figure S19. Computed eigenvalue plot incorporating energies computed for d-based orbitals for alpha and beta spin corresponding to the ground state $^3Cu_{hs}$ of the copper(III) hydroperoxo species (energies are given in eV).

³Cu_hs

$d_{xy}(0.01e^-)$ $d_{xz}(0.01e^-)$ $d_{yz}(0.01e^-)$ $d_{x^2-y^2}^2(1.00e^-)$

$d_{z^2}^2(1.00e^-)$ $d_{xy}(-0.01e^-)$ $d_{xz}(-0.01e^-)$ $d_{yz}(-0.01e^-)$

³Cu_hs-ts

$d_{xy}(0.01e^-)$ $d_{xz}(0.01e^-)$ $d_{yz}(0.01e^-)$ $d_{x^2-y^2}^2(1.00e^-)$

$d_{z^2}^2(1.00e^-)$ $d_{xy}(-0.01e^-)$ $d_{xz}(-0.01e^-)$ $d_{yz}(-0.60e^-)$
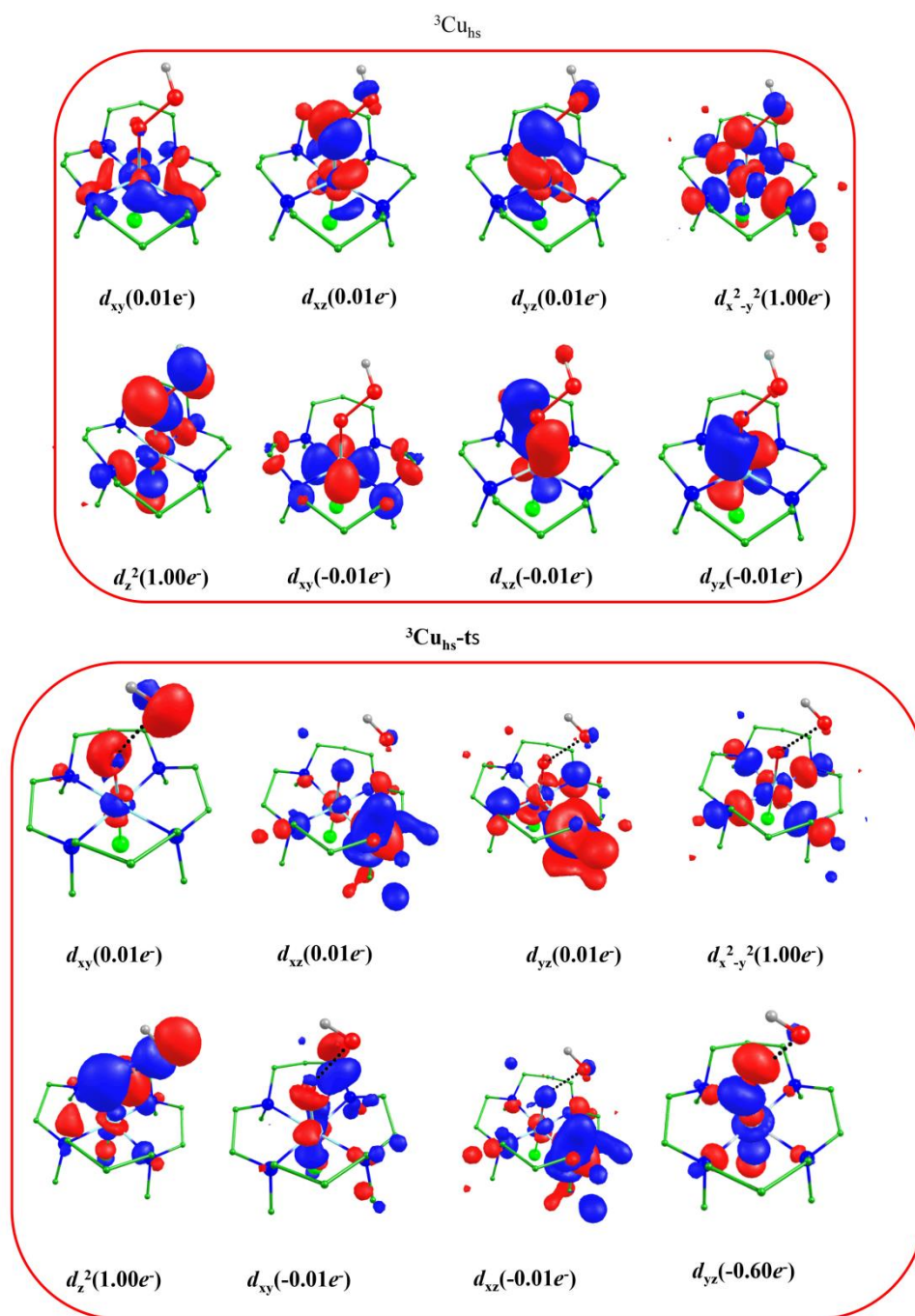
Figure S20. Spin natural orbitals and their occupations (noted in parenthesis) of ⁵Cu_hs, and ⁵Cu_hs-ts.
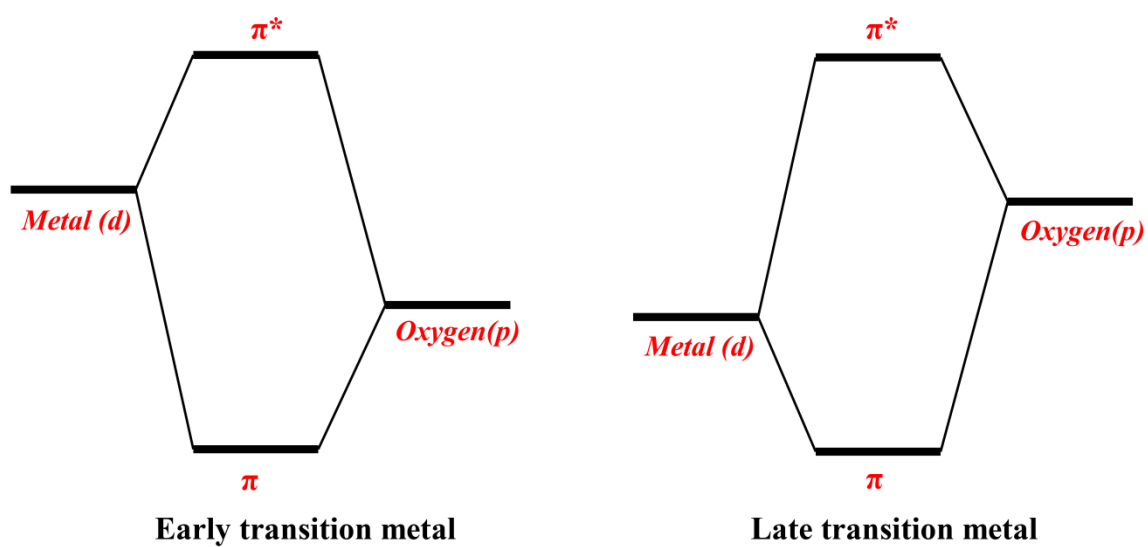
Scheme S2. Pi interaction of the metal *d* orbitals with that of the oxygen *p* orbitals.

Table S5. Computed stretching frequency of M-O bond in Metal-oxo species

| Metal-oxo	v (cm^{-1})
^{3}Cr$_{hs}$-Int	558
^{4}Mn$_{hs}$-Int	869
^{5}Fe$_{hs}$-Int	872
^{4}Co$_{is}$-Int	849
^{5}Ni$_{hs}$-Int	499
^{4}Cu$_{hs}$-Int	376
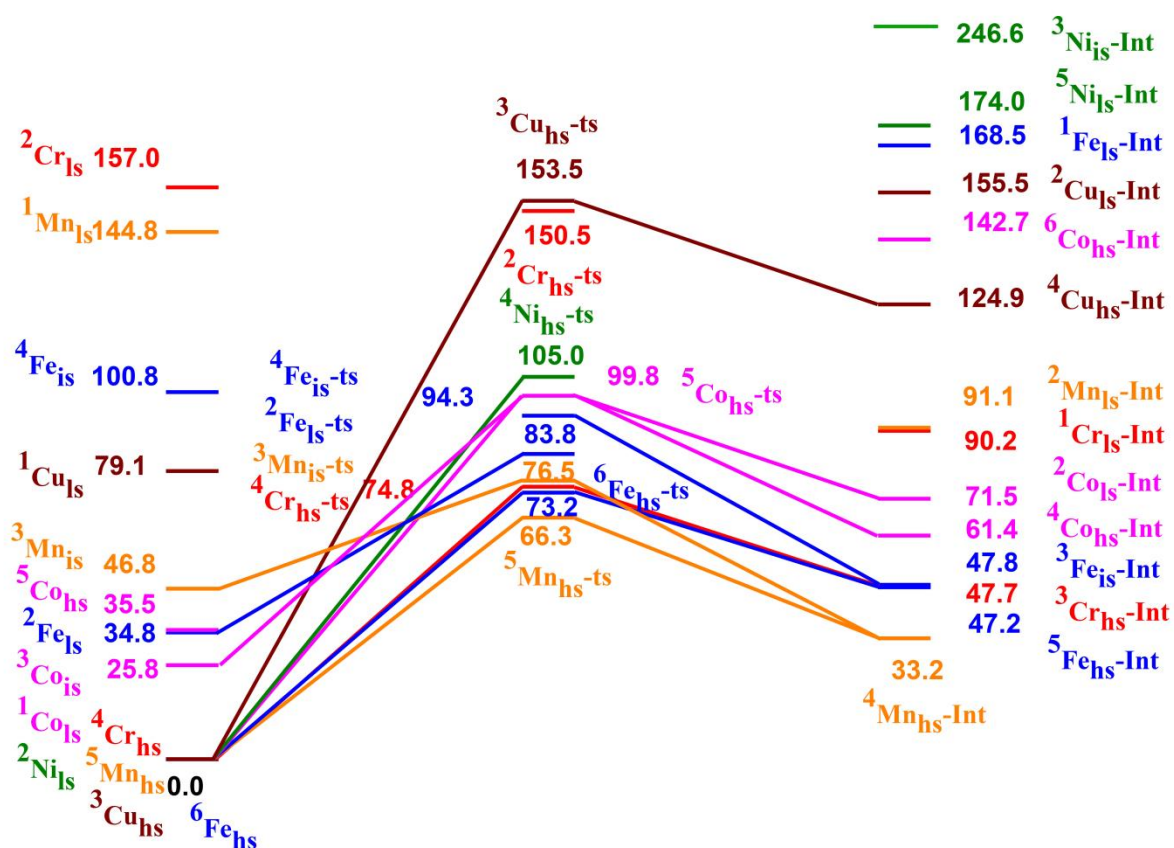
Figure S21. B3LYP-D2 computed energy surface for the formation of metal-oxo from 14-TMC metal hydroperoxo chromium (red), manganese (orange), iron (blue), cobalt (purple), nickel (green), and copper (dark red).

References

1. J. Cho, J. Woo and W. Nam, *J. Am. Chem. Soc.*, 2012, **134**, 11112-11115.

2. J. U. Rohde, J. H. In, M. H. Lim, W. W. Brennessel, M. R. Bukowski, A. Stubna, E. Münck, W. Nam and L. Que Jr., *Science*, 2003, **299**, 1037-1039.

3. B. Wang, Y. M. Lee, W. Y. Tcho, S. Tussupbayev, S. T. Kim, Y. Kim, M. S. Seo, K. B. Cho, Y. Dede, B. C. Keegan, T. Ogura, S. H. Kim, T. Ohta, M. H. Baik, K. Ray, J. Shearer and W. Nam, *Nat Commun.*, 2017, **8**, 14839-14849.

4. H. Hirao, D Kumar, L. Que, Jr. and S Shaik, *J. Am. Chem. Soc.,* 2006, **128**, 8590-8606.